Polymer 51 (2010) 4448–4451

Contents lists available at ScienceDirect

Polymer

journal homepage: www.elsevier.com/locate/polymer

Molecular modeling of particle reinforcement in elastomers: Effect of particle radius and volume fraction

Yves Termonia

Central Research and Development, DuPont Nanocomposite Technologies, Building E304, Room C219, Experimental Station, E.I. DuPont de Nemours, Inc. Wilmington, DE 19880-0304, United States

ARTICLE INFO

Article history:
Received 15 June 2010
Received in revised form
16 July 2010
Accepted 20 July 2010
Available online 30 July 2010

Keywords:
Nanoparticle simulation modulus

ABSTRACT

Monte-Carlo simulations of the configurations of polymer chains in reinforced elastomers reveal extensive wrapping of the chains around particle clusters. The resulting increase in chain entanglement density leads to a 3.5 power law dependence of modulus on particle loading, in perfect agreement with experimental observation. Our model also gives a consistent molecular explanation of the Payne effect and the associated energy dissipation in strained reinforced elastomers.

1. Introduction

For more than a century now, spherical particles such as carbon black and silica have been extensively used to reinforce elastomers and improve their modulus and abrasion resistance. In spite of extensive research in the area, the origin of that reinforcement still remains under debate. Also poorly understood is the associated Payne effect [1] under cyclic loading, *i.e* a decrease in modulus with strain, which is not observed for unfilled elastomers.

Several theories have been proposed for describing the properties of filled elastomers. In a first approach, the reinforcement is attributed to particle–particle interactions within large percolating clusters with no contributions from the elastomeric phase [2–4]. The Payne effect is then attributed to the breaking of weak bonds between particles. That interpretation has been disputed by Sternstein and Zhu [5] who observed the Payne effect at loadings below percolation. The second approach invokes strong polymer–particle interactions [6–8]. That theory correctly accounts for the increase of modulus with polymer molecular weight as the chains form long-lived bridges between the particles which behave as high functional crosslinks. The origin of the reinforcement with gel particles having weak interactions with the polymer however remains unaccounted for. A third set of theories attribute elastomer reinforcement to the presence of a “glassy” polymer shell at the interface with the particles [9,10]. That interpretation -again- does not explain the dependence of the composite modulus on polymer molecular weight nor the observation of a Payne effect at high temperatures above the polymer glass transition temperature [8].

In the present work, we present results of a Monte-Carlo (MC) study of the configuration of long chains around agglomerates of spherical particles in an *uncured* elastomer. The effect of crosslinking on our model results will be discussed towards the end of the paper. The agglomerates are generated using a cluster–cluster aggregation (CCA) model [11] which describes particle evolution in such systems [12]. For simplicity, we assume no particle–polymer interactions.

2. Model

In our approach, the ensemble of particles and polymer chains is generated on a simple cubic lattice with periodic boundary conditions and unit length ℓ equal to the statistical segment length for the chains. We start by randomly generating on the lattice an array of spherical particles of radius $r \geq \ell/2$ for a volume fraction φ. In the CCA algorithm, the centers of mass of the particles move to nearest neighbor sites and stick upon contact with neighbor particles. After a few iterations, one quickly obtains a collection of clusters. Each of these clusters then moves according to its diffusion coefficient, *i.e.*with probability [11]

$$p_i = R_{g,i}^{-1} \Big/ \sum R_{g,i}^{-1} \tag{1}$$

in which $R_{g,i}$ is the radius of gyration of cluster i. For simplicity, rotations of the clusters around their centers of mass are not allowed. If the move leads to collision with another cluster, the

E-mail address: yves.termonia@usa.dupont.com.

0032-3861/$ – see front matter © 2010 Elsevier Ltd. All rights reserved.
doi:10.1016/j.polymer.2010.07.029

collection of clusters is updated: the two colliding clusters are discarded and replaced by a single one.

The lattice containing the clusters is then filled in with a dense array of long flexible polymer chains with high density $\rho = 0.92$. Unoccupied lattice sites are considered as vacancies. Note that lower ρ values will decrease the density of chain entanglements in the bulk and the findings -to be discussed later- will be less pronounced. Our technique follows that of Refs.[13,14], which is very briefly recapitulated here. Initially, the chains are in an ordered and folded conformation. They are then equilibrated using elementary moves of two types. The first set of moves involves elementary rotations of a kink, a crankshaft or a chain end into a vacancy. The second set of moves involves exchanges of crankshaft segments between chain strands at adjacent positions. Full equilibrium is considered to be achieved when the average values of the radius of gyration for the chains and the eigenvalues of their gyration tensor approach steady state values.

All our results are for large lattices of $60 \times 60 \times 60$ sites and a constant chain length $N = 761$ ℓ, which lies above the critical value for entanglement behavior in the unfilled polymer [14]. Unless otherwise noted, all our results are for particle aggregation through Brownian motion (*vs.* ballistic motion in which particles follow straight trajectories).

3. Results and discussion

The conformations of the polymer chains in our particle systems can be conveniently studied through an analysis of their primitive path [15,16]. The latter represents the shortest path between the endpoints of a chain into which its contour can be contracted without crossing any obstacle. For a polymer–particle system, these obstacles can be either another polymer chain or a cluster of particles. Within the framework of our approach, the primitive path is obtained by first fixing the chain ends in space. The chains are then relaxed through a series of kink rotations while at the same time shortening their contour length [14] between the fixed ends. That shortening was obtained through systematically cutting crankshaft units which leave behind pairs of vacancies. Our process effectively makes the chains taut between the fixed chain ends and successive entanglements appear as kinks linked through straight contour lines. The average number N_e of chain segments between kinks is obtained through [14]

$$N_e = N < R_{ee}^2 > / < L_p^2 > \quad (2)$$

in which the averages are calculated over all the chains, whereas R_{ee} and L_p denote the lengths of the end-to-end vector and contour of the primitive path. Within the framework of the primitive path method, Eq.(2) effectively calculates the number of chain segments between entanglements.

Fig. 1 (open symbols) shows the calculated dependence of N_e on the volume fraction of particles for $r = 0.5$ ℓ. The dashed line is drawn to guide the eye. Our data are for various extents of aggregation ranging from partial aggregation with an average number of particles per cluster around 20 to full aggregation into a single cluster. Data with symbol △ are for the special case of ballistic aggregation. The figure clearly reveals that our N_e values can be considered to be independent of the mode and extent of aggregation. Our data also indicate a fast decrease in N_e, *i.e* increase in the density of entanglements, with the particle volume fraction. In an effort to separate chain–chain from chain-particle entanglements, we have also plotted in Fig. 1 (full symbols) our N_e values obtained for the case when, before the start of the primary path construction, the particles are removed and replaced with vacancies. These simulations reveal an *increase* in N_e at $\varphi > 0.28$. The implications are two-fold:

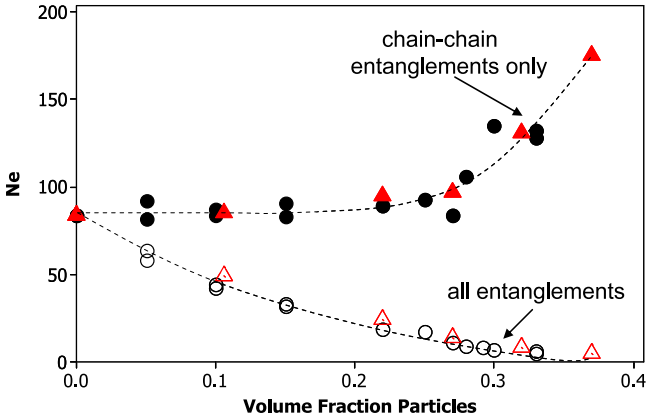

Fig. 1. Dependence of the number of chain segments between entanglements, N_e, on the volume fraction of particles with radius $r = 0.5$ ℓ (open symbols). The data are for various extents of aggregation ranging from partial aggregation with an average number of particles per cluster around 20 to full aggregation into a single cluster. The full symbols are for chain–chain entanglements only. Values of N_e obtained for the case of ballistic particle aggregation are denoted with red triangles (▲ and △). The dashed lines are drawn to guide the eye.(For interpretation of the references to colour in this figure legend, the reader is referred to the web version of this article).

(1) The particles act as a diluent for the chains which are also swollen [14]. At a critical $\varphi > 0.28$, swelling leads to chain–chain disentanglement. No change in entanglement density is observed at very low dilutions $\rho < 0.2$.

(2) The decrease in N_e observed earlier for the full system (chains + particles) is due to chain entanglements around particles. This is clearly illustrated in Fig. 2 which shows the primitive paths of two chains (taken out of a dense melt) near a cluster of fully aggregated particles with $r = 0.5$ ℓ and at very low $\varphi = 0.005$ for ease of visualization. One chain (red) is seen to entangle both with the other one (blue) and with the cluster of particles. Our findings support the chain–particle entanglement hypothesis advanced by Zhang & Archer [6] to explain their viscosity data for poly(ethylene oxide)-silica nanocomposites.

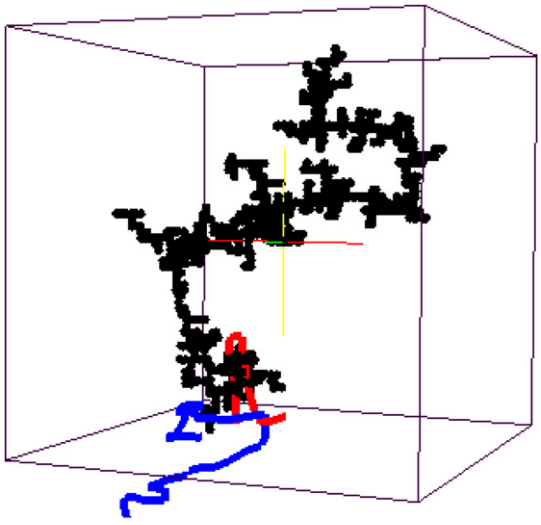

Fig. 2. Primitive paths of two chains (taken out of a dense melt) around a cluster of fully aggregated particles with $\phi = 0.005$ and $r = 0.5$ ℓ. One chain (red) is seen to entangle both with the other one (blue) and with the cluster.(For interpretation of the references to colour in this figure legend, the reader is referred to the web version of this article).

Using Eq.(2), an estimation of the modulus is easily obtained from [17]

$$G \sim 1/N_e \tag{3}$$

Our results for the dependence of G on the volume fraction of particles, φ, are presented in Fig. 3. The figure is for different values of the particle radius r (in units of ℓ). Data represented by the open red triangles (△) at $r = 0.5$ are for the case of ballistic particle aggregation. The lines are drawn to guide the eye. Our results indicate that, at a critical value of φ which increases with r, the modulus increases sharply with a scaling law $G \sim \varphi^{3.5}$. Note also that, at $r = 0.5$, scaling occurs well below the critical value $\varphi_c = 0.311$ for site percolation on the simple cubic lattice [18]. Turning to comparison with experimental data, our scaling exponent is in perfect agreement with that obtained for elastomer reinforcement with carbon black, silica and microgel particles [19]. Our finding of a delayed reinforcement at large r also agrees with data on carbon blacks [20] and PS microgel particles [21] of various sizes. Note however that the experimental data of Refs.[20,21], are for particle radii around 10 nm. Since, in our simulations $\ell \approx 1$ nm [13,14], these radii values are larger than those at which we predict reinforcement. We believe that the origin of that discrepancy lies in the fact that, in order for chain–particle entanglements to form, the radius of gyration of the chains, R_g, must be substantially larger than the particle radius. This is the case for our data of Fig. 3 since $R_g = 11.7\ \ell$ [13,14]. In crosslinked elastomers however, the "effective" R_g is much larger than that of the individual chains and reinforcement can be observed at higher particle radii.

We now turn to comparison of the present model to others [2–4] which attribute reinforcement solely to percolating clusters of particles. Analytical theories of the elasticity of these clusters [22,23] have led to scaling laws for the dependence of G on φ with exponent values similar to ours and also in agreement with experiment. However, in contrast to our approach, these theories are unable to address any role of the polymer molecular weight [6]. Nor can they predict an increase in modulus at lower particle radius. In order to correct for the latter, a dependence on particle size has been introduced [23] through a mechanically "effective" solid fraction of the clusters which includes the effect of a hard glassy layer of immobilized polymer around the particles. Another major difference between our model and that of Refs.[22,23] lies in their explanations of the Payne effect and the accompanying excess energy loss. Thus, particle cluster theories describe the deformation dependence of the modulus of filled elastomers through a progressive breakdown of the clusters. However, in all cases, additional assumptions have to be made about the accompanying high energy dissipation. In our approach, the decrease in modulus in a strained elastomer is rationalized though a *decrease in chain entanglement density*. The latter can occur either through breakdown of particle clusters near chain–particle entanglements and/or through chain slippage and disentanglement near dangling ends. The decrease in entanglement density leads to chain recoil and to a loss in elastic stored energy which readily accounts for the markedly enhanced energy dissipation in reinforced elastomers.

We now turn to show how a process of disentanglement through chain slippage affects the deformation behavior of an elastomer in a manner entirely consistent with experimental observations of the Payne effect. Our study is based on previous work [24,25] and a schematic representation of our model is given in Fig. 4. The network consists of a random array of linear chains which interact at nodes placed on a regular two-dimensional lattice. These nodes represent either crosslinks or entanglements. Without any loss in generality, only chain–chain entanglements are being considered. The network is strained at a constant temperature T and rate $d\varepsilon/dt$. For every strain increment $\delta\varepsilon$, every node is relaxed towards mechanical equilibrium with its connected neighbors. The stress σ on a particular chain strand between two nodes is assumed to be Gaussian and is calculated using

$$\sigma = \alpha kT3[(r/nl) - \sigma_0] \tag{4}$$

in which α has the dimensions of an inverse volume [24], n denotes the number of statistical segments of length ℓ and r is the distance between the nodes. In Eq.(4), σ is decreased by its value σ_o at zero strain, *i.e.* for which $r = n^{1/2}\ell$. Because of the presence of chain ends, deformation occurs in a non-affine manner which creates increasing stress gradients on chains passing through entanglements. These gradients lead to chain slippage which occurs at a rate [24]

$$\nu = \tau \exp[-(U - \beta\Delta\sigma)/kT] \tag{5}$$

in which τ is a thermal vibration frequency whereas U and β denote an activation energy and volume. Our calculated stress–strain curves at various strain rates (in sec^{-1}) are presented in Fig. 5. The results are for chains with 20 nodes along their contour and $n = 6$ segments between nodes. The nodes are divided among crosslinks and entanglements in the ratio 4/6. In Eqs.(4,5), we took $\tau = 10^{12}$/sec, $U = 20$Kcal/mol, $\alpha = 2.4 \times 10^{26}/m^3$ [24] and $\beta\alpha = 2.66$. Inspection of our results of Fig. 5 reveals that the stress–strain curves exhibit two

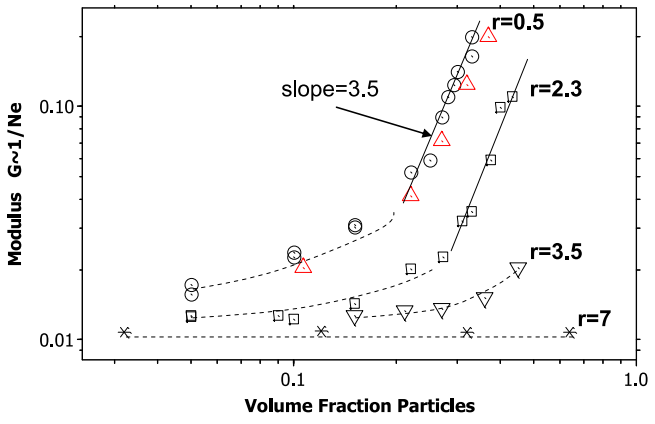

Fig. 3. Dependence of the modulus $G \sim 1/N_e$ on the volume fraction of particles. The data are for different values of the particle radius r (in units of ℓ). Values of N_e at $r = 0.5$ represented by the open red triangles (△) are for the case of ballistic particle aggregation. The lines are drawn to guide the eye.(For interpretation of the references to colour in this figure legend, the reader is referred to the web version of this article).

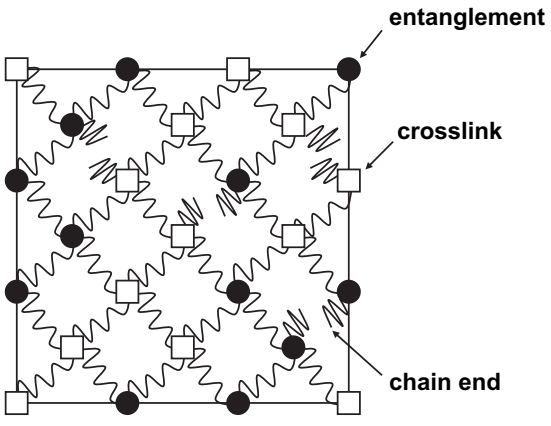

Fig. 4. Schematic lattice representation of a crosslinked elastomeric network.

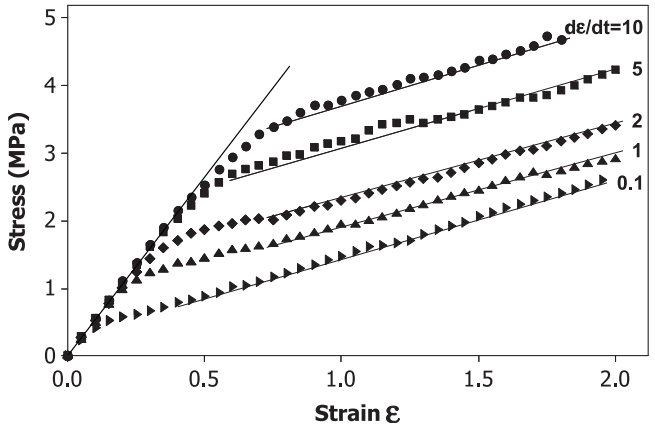

Fig. 5. Stress–strain curves at various strain rates dε/dt (in sec^{-1}) for the model of Fig. 4. The data are for chains with 20 nodes along their contour and $n = 6$ segments between nodes. The nodes are divided among crosslinks and entanglements in the ratio 4/6. In Eqs. (4,5), we took $\tau = 10^{12}$/sec, $U = 20$Kcal/mol, $\alpha = 2.4 \times 10^{26}/m^3$ [25] and $\beta\alpha = 2.66$.

different regimes. At low strains ε, all the curves have a high modulus value which is weakly dependent on rate. As ε increases, the modulus starts to decrease towards a lower value which is identical for all curves. The rate of deformation, dε/dt, appears to affect only the critical strain value ε_c at which the modulus decreases. The lower dε/dt, the smaller ε_c. Further investigation of our model results reveals that the modulus decrease is due to slippage of chains through entanglements. That process is exacerbated at low dε/dt and it subsides when all the chain entanglements which are not trapped between crosslinks have been lost. Note also that, within the framework of our model, the decrease in modulus in Fig. 5 is expected to be completely recovered with time upon release of the external strain. Finally, turning to comparison with experiment, our calculated stress–strain curves are strikingly similar to those observed for silicone elastomers filled with silica particles [26]. A last remark is in order. Our approach assumes no enthalpic interactions between polymer and particles. In the presence of attractive interactions, it is expected that chain slippage through particle–polymer entanglements will be hindered and hence the Payne effect should be less pronounced.

In summary, a Monte-Carlo study of the configurations of polymer chains in reinforced elastomers reveals extensive wrapping of the chains around particle clusters. The resulting increase in chain entanglement density leads to a 3.5 power law dependence of the modulus on particle loading, in perfect agreement with experimental observation. Our results also clearly indicate a decrease in reinforcement efficiency with an increase in particle radius. Finally, using a kinetic approach developed previously [24,25], we find that chain disentanglement affects the deformation behavior of a reinforced elastomer in a manner entirely consistent with experimental observations of the Payne effect.

References

[1] Payne AR. Rubber Chem Technol 1963;36:432–5.
[2] Lin CR, Yee YD. Macrom Theory Simul 1996;5:1075–104.
[3] Rong W, Ding W, Madler L, Ruoff RS, Friedlander SK. Nanoletters 2006;6:2646–9.
[4] Heinrich G, Kluppel M, Vilgis TA. Curr Opin Solid State Mater Sci 2002;6:195–203.
[5] Sternstein SS, Zhu AJ. Macromolecules 2002;35:7262–73.
[6] Zhang Q, Archer LA. Langmuir 2002;18:10435–42.
[7] Yurekli K, Krishnamoorti R, Tse MF, McElrath KO, Tsou AH, Wang H-C. J Polym Sci 2001;B39:256–75.
[8] Zhu Z, Thompson T, Wang S-Q, von Meerwall ED, Halasa A. Macromolecules 2005;38:8816–24.
[9] Berriot J, Montes H, Lequeux F, Long D, Scotta P. Macromolecules 2002;35:9756–62.
[10] Montes H, Lequeux F, Berriot J. Macromolecules 2003;36:8107–18.
[11] Meakin P. Annu Rev Phys Chem 1988;39:237–56.
[12] Kluppel M. Adv Polym Sci 2003;164:1–86.
[13] Termonia Y. Polymer 2009;50:1062–6.
[14] Termonia Y. J Polym Sci Part B Polym Phys 2010;48:687–92.
[15] Everaers R, Sukumaran SK, Grest GS, Svaneborg C, Sivasubramanian A, Kremer K. Science; 2004:303–823.
[16] Tsoumanekas C, Theodourou DN. Macromolecules 2006;39:4592–604.
[17] Treloar LRG. The physics of rubber elasticity. 2nd ed. Oxford: Clarendon; 1958.
[18] Stauffer D. Phys Rep 1979;54:1–74.
[19] Heinrich G, Kluppel M, Vilgis T. In: Mark JE, editor. Physical properties of polymers handbook. 2nd ed. NY: Springer; 2007. pp. 599–608 [chapter 36].
[20] Donnet JB, Vidal A. In: Dusek K, editor. In pharmacy/thermomechanics/elastomers/telechelics. Berlin: Springer-Verlag; 1986. pp. 104–127.
[21] Bischoff A, Kluppel M, Schuster RH. Polym Bull 1998;40:283–90.
[22] Kantor Y, Webman I. Phys Rev Lett 1984;52:1891–4.
[23] Kluppel M, Schuster RH, Heinrich G. Rubber Chem Technol 1997;70:243–53.
[24] Termonia Y, Smith P. Macromolecules 1987;20:835–8.
[25] Termonia Y. Macromolecules 1989;22:3633–8.
[26] Chazeau L, Brown JD, Yanyo LC, Sternstein SS. Polym Compos 2000;21:202–22.